16th World Conference on Earthquake, 16WCEE 2017

Santiago Chile, January 9th to 13th 2017

Paper N° 2943 (Abstract ID)

Registration Code: S-XXXXXXXX

DAMAGE INDICES FOR LOAD-BEARING CAPACITY AND STIFFNESS OF FIRE-DAMAGED WALLS

S. Ni[(1)], A.C. Birely[(2)]

[(1)] *Graduate Research Assistant, Zachry Department of Civil Engineering, Texas A&M University, nishuna@tamu.edu*
[(2)] *Assistant Professor, Zachry Department of Civil Engineering, Texas A&M University, abirely@civil.tamu.edu*

Abstract

Experimental and numerical studies have shown that fire damage negatively influences the seismic performance of reinforced concrete structural members. This paper investigates damage indices that quantify the influence of fire damage on the lateral stiffness and the lateral-load bearing capacity of RC structural walls. The damage indices are based on the fire damaged material properties of concrete and reinforcing steel for the wall section, and are on a scale ranging from zero to unity, where unity represents the undamaged state of a wall section. The post-fire seismic performance of sixteen RC structural walls are analyzed using a validated simulation method under sequential fire-earthquake loads. The numerical load-bearing capacity and stiffness of walls under lateral loads and the damage indices of wall sections are calculated. Preliminary relationships between the damage indices and the numerical post-fire seismic performance of RC structural walls are established. Those proposed relationships help in assessing the post-fire performance of RC structural walls based on the damage indices.

Keywords: multi-hazard; reinforced concrete; structural walls

1. Introduction

Various methods are available for the assessment of fire damage to concrete structures, including visual inspection, non-destructive testing and partially-destructive testing. In the visual inspection, fire damage to a concrete structure is estimated by observing finishes, color, crazing, spalling cracks and deflections (Ellsworth and Ginnado, 1991). The non-destructive testing methods of fire-damaged concrete includes ultrasonic pulse velocity technique, ultrasonic-rebound combined method and infrared thermal imaging et al. (Dilek, 2007; Colombo and Felicetti, 2007). The partially-destructive testing methods include rebound hammer, probe penetration, pull-off et al. (Bungey and Soutsos, 2001). All of those methods estimate the fire damage to material, not the performance of a structure or a structural member. However, those methods make the test of fire-damaged material properties of fire-damaged concrete and fire-damaged reinforcing steel easy. Therefore, if the relationships between the fire-damaged material properties and residual performance (strength, stiffness, ductility and failure drift) of a fire-damaged RC structural member are established, it is not difficult to determine the residual capacity of a fire-damaged RC structural member by the available material data.

Fire design codes (EC2-04 and ACI 216.1-97) and research (Anderberg and Holmberg, 1993; Franssen et al., 1996; Lie and Irwin, 1993) have proposed simplified methods to calculate the ultimate strength of reinforced concrete members at elevated temperature. For example, two simplified methods presented in EC2-04 are 1) 500^{o}C isothermal method and 2) zone method. Those methods are based on the variation of material strength with temperature and calculate the ultimate strength of reinforced concrete members at elevated temperature based on reduced section, which further indicates that fire damage to materials plays an important role in estimating the performance of a structure in a fire or after a fire. Therefore, damage indices based on the residual material properties may well represent the damage levels of a RC structural member after fire exposure.

This paper focuses on the performance assessment of fire-damaged reinforced concrete (RC) structural walls. The use of reinforced concrete structural walls in buildings is a very popular scheme in the design of multistory buildings to resist lateral loads. Another important function of structural walls is that they may serve as fire walls to suppress the spread of fire in the horizontal direction. When a building with RC structural walls as the main lateral-load resisting system is damaged in fire, it is important to estimate the residual performance of RC structural walls under lateral load before any repair work is conducted. In this paper, fire damage indices for the load-bearing capacity and stiffness of RC structural walls under lateral loads are proposed based on the fire-damaged material properties of concrete and reinforcing steel. Numerical analysis of fire-damaged walls under lateral loads was conducted. The values quantifying the damage indices and the wall performance were calculated. The relationships between the damage indices and the loading-bearing capacity and lateral stiffness of RC structural walls were developed. Those damage indices are intended to provide engineers with a quick method to estimate the post-fire seismic performance of RC structural walls.

2. Description of simulation method

The post-fire seismic performance of flexure-controlled reinforced concrete were analyzed by a simulation procedure combining heat transfer analysis in SAFIR and seismic analysis in OpenSees (Ni and Birely, 2015). In this simulation procedure, SAFIR (Franssen, 2011) was used for the heat transfer analysis of wall sections while OpenSees (Mazzoni et al., 2006) was used for the seismic analysis of walls under reversed-cyclic lateral loads. The heat transfer analysis determines the maximum temperature each fiber has experienced in the heating-cooling cycle. MATLAB codes were written to modify the material properties of each fiber for the post-fire seismic analysis according to the maximum temperature. In the seismic analysis, the flexural and axial response of the walls was modeled using fiber sections followed the recommendations of Pugh (2012), which were validated for simulation of flexural-controlled planar walls using an extended data set; no shear deformation was considered in the simulation. The fiber elements used in the analysis were force-based beam-column elements. The whole simulation procedure is shown in Fig. 1. After the lateral load-drift response of walls under reversed-cyclic loads was obtained, the following key response quantities were calculated: The lateral load capacity, V_{max} is the maximum lateral load a wall experiences before its lateral loading capacity begins to decrease. $V_{max,fire}$ is the fire-reduced lateral load capacity of a fire damaged wall and $V_{max,0}$ is the lateral load capacity of an undamaged wall. The stiffness up to yield, K_{sec} is a secant stiffness, defined by the lateral load at yield divided by the displacement at yield. $K_{sec,fire}$ is the stiffness up to yield of a fire-damaged wall and $K_{sec,0}$ is the stiffness up to yield of a undamaged wall.

Table 1 lists the flexure-controlled walls tested by other research under reversed-cyclic loads at room temperature and fail in flexure pattern. The post-fire seismic performance of the walls were investigated numerically, using the simulation procedure in Fig.1. Four different thermal boundary conditions were considered, shown in Fig.2. The thermal parameters for the boundaries are as followings: the emissivity coefficient ε_r is 0.7; the film coefficient h_c is 25 W/m^{2}K for the fire-exposed side and h_c is 9W/m^{2}K for the fire-unexposed side (exposed to room temperature). Walls in Table 1 were heated by ASTM E119 fire curves in the heating phase with different fire durations and were cooled down at 0.5^{o}C/min in the cooling phase. After the heating-cooling cycle, the post-fire seismic performance of the walls were analyzed.

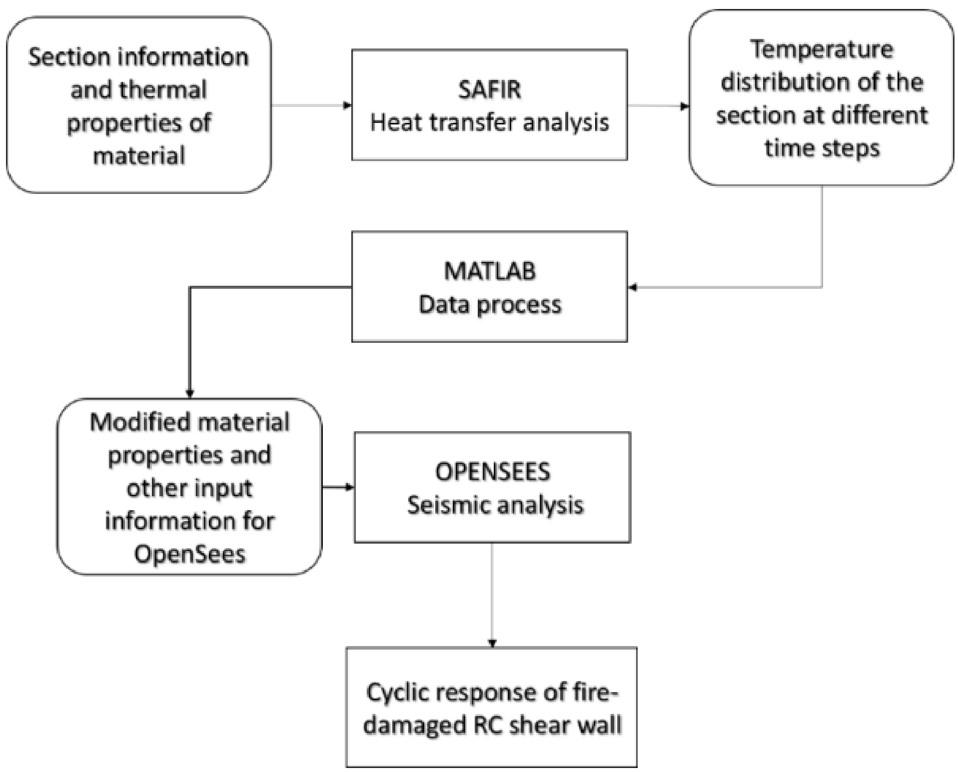

Fig. 1- Interaction between SAFIR and OpenSees

Table 1 – Flexure-controlled RC structural walls

Author	Specimens	$M_b/(V_b l_w)$	Thickness (mm)
Dazio et al. (2009)	WSH1-WSH5	2.28	150
Dazio eta al. (2009)	WSH6	2.26	150
Liu (2004)	W1	3.13	200
Lowes et al. (2012)	PW1	2.84	152
Lowes et al. (2012)	PW2-PW4	2	152
Oh et al. (2002)	WR20, WR10, WR0	2	200
Thomsen et al. (2004)	RW1, RW2	3.13	102

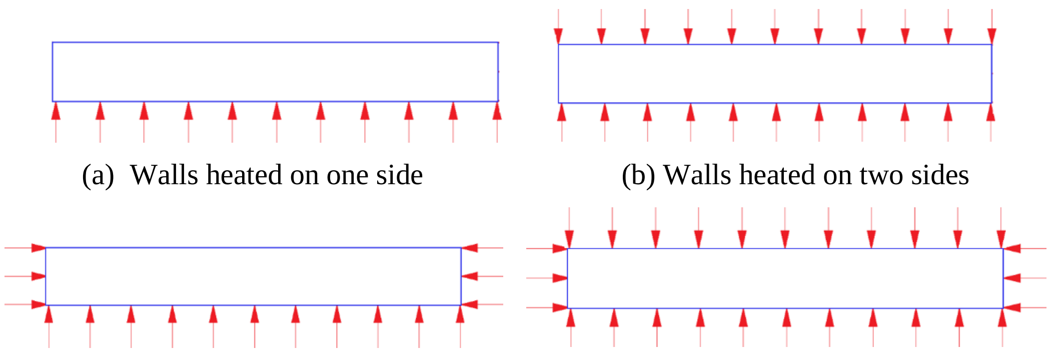

(a) Walls heated on one side (b) Walls heated on two sides

(c) Walls heated on three sides (d) Walls heated on four sides

Fig. 2 – Thermal boundary conditions
(Arrows indicate heated sides and other sides are exposed to room temperature)

3. Definition of Damage indices for the strength and stiffness of walls

As mentioned in the introduction, it is possible to test the fire-damaged material properties of concrete and reinforcing steel. The damage indices presented below are based on the fire-damaged material properties of concrete and reinforcing steel. Two kinds of damage indices are defined: the damage index of strength (DIS) and the damage index of elastic modulus (DIEM). DIS represents the damage level of a wall in lateral load-bearing capacity and is calculated using the residual material strength of the fire damaged wall section. DIEM represents the damage level of a wall in lateral stiffness and is calculated using the residual elastic modulus of material in the fire damaged wall section. Four sets of definitions are considered. The first two consider concrete contributions only, while the last incorporate characteristics of the steel as well. The first and third definitions treat all concrete equally while the second and third consider the different characteristics of confined and unconfined concrete.

Definition 1: in Definition 1, both DIEM and DIS are only based on the post-fire material properties of concrete and the influence of confining effect and the contribution of reinforcing steels are not considered.

$$\mathrm{DIS1} = \frac{\sum A_{ci} f_{ci,r}}{A_o f_{c,0}} \tag{1}$$

$$\mathrm{DIEM1} = \frac{\sum A_{ci} E_{ci,r}}{A_o E_{c,0}} \tag{2}$$

Where A_{ci} is the area of the concrete fiber i; $f_{ci,r}$ is the residual compressive strength of concrete fiber i; A_o is the total area of concrete fibers (including the confined concrete and the unconfined concrete) and $f_{c,o}$ is the compressive strength of concrete at room temperature; $E_{ci,r}$ is the residual elastic modulus of concrete fiber i; $E_{c,0}$ is the elastic modulus of concrete fiber i at room temperature.

Definition 2: Since the performance of walls under lateral load is influenced significantly by the confined boundary region, both DIS and DIEM consider the influence of the confining effect in the boundary región in this definition.

$$\mathrm{DIS2} = \frac{\sum A_{ci} f_{ci,r} + \sum A_{cci} f_{cci,r}}{A_c f_{c,0} + A_{cc} f_{cc,0}} \tag{3}$$

$$\mathrm{DIEM2} = \frac{\sum A_{ci} E_{ci,r} + \sum A_{cci} E_{cci,r}}{A_c E_{c,0} + A_{cc} E_{cc,0}} \tag{4}$$

Where A_{cci} is the area of the confined concrete fiber i; A_c is the total area of unconfined concrete; A_{cc} is the total area of confined concrete; $f_{cci,r}$ is the residual compressive strength of confined concrete fiber i; $f_{cc,o}$ is the compressive strength of confined concrete at room temperature; $E_{cci,r}$ is the residual elastic modulus of confined concrete fiber i; $E_{cc,0}$ is the elastic modulus of confined concrete at room temperature.

Definition 3: in Definition 3, both DIEM and DIS consider the contribution of reinforcing steel, in addition to that of all concrete fiber without the confining effect considered.

$$\mathrm{DIS3} = \frac{\sum A_{ci} f_{ci,r} + \sum A_{si} f_{syi,r}}{A_c f_{c,0} + A_{sb} f_{sby} + A_{sw} f_{swy}} \tag{5}$$

$$\mathrm{DIEM3} = \frac{\sum A_{ci} E_{ci,r} + \sum A_{si} E_{si,r}}{A_c E_{c,0} + A_{sb} E_{sb} + A_{sw} E_{sw}} \tag{6}$$

Where A_{si} is the area of steel fiber i in a wall section; A_{sb} is the total area of the longitudinal reinforcing steel in the boundary region; A_{sw} is the total area of the longitudinal reinforcing steel in the web region; $f_{syi,r}$ is the residual yield strength of steel fiber i; f_{sby} is the yield strength of the longitudinal reinforcing steel in the boundary region at room temperature; f_{swy} is the yield strength of the longitudinal reinforcing steel in the web region at room temperature; $E_{si,r}$ is the residual elastic modulus of steel fiber i; E_{sb} is the elastic modulus of the longitudinal reinforcing steel in the boundary region at room temperature; E_{sw} is the elastic modulus of the longitudinal reinforcing steel in the web region at room temperature.

Definition 4: In Definition 4, the influence of reinforcing steel on the lateral performance of walls is incorporated into the damage indices, in addition to the contribution of the confining effect of boundary región.

$$\mathrm{DIS4} = \frac{\sum A_{ci} f_{ci,r} + \sum A_{cci} f_{cci,r} + \sum A_{si} f_{syi,r}}{A_c f_{c,0} + A_{cc} f_{cc,0} + A_{sb} f_{sby} + A_{sw} f_{swy}} \tag{7}$$

$$\mathrm{DIEM4} = \frac{\sum A_{ci} E_{ci,r} + \sum A_{cci} E_{cci,r} + \sum A_{si} E_{si,r}}{A_c E_{c,0} + A_{cc} E_{cc,0} + A_{sb} E_{sb} + A_{sw} E_{sw}} \tag{8}$$

Fig.3(a) shows the maximum temperature of each fiber in the section of wall specimen WR20. Fig.3(b) shows the residual strength of each fiber in the section of wall specimen WR20. Fig.3(c) shows the residual elastic modulus of each fiber in the section of wall specimen WR20. The thermal boundary condition for this case is shown in Fig.2(c) and different fire durations of the heating phase were considered (fifteen-minute fire, half-an-hour fire, one-hour fire, two-hour fire and three-hour fire and four-hour fire). According to the residual material properties, DIS and DIEM for each wall in Table 1 under fire with different durations and thermal boundary conditions were calculated.

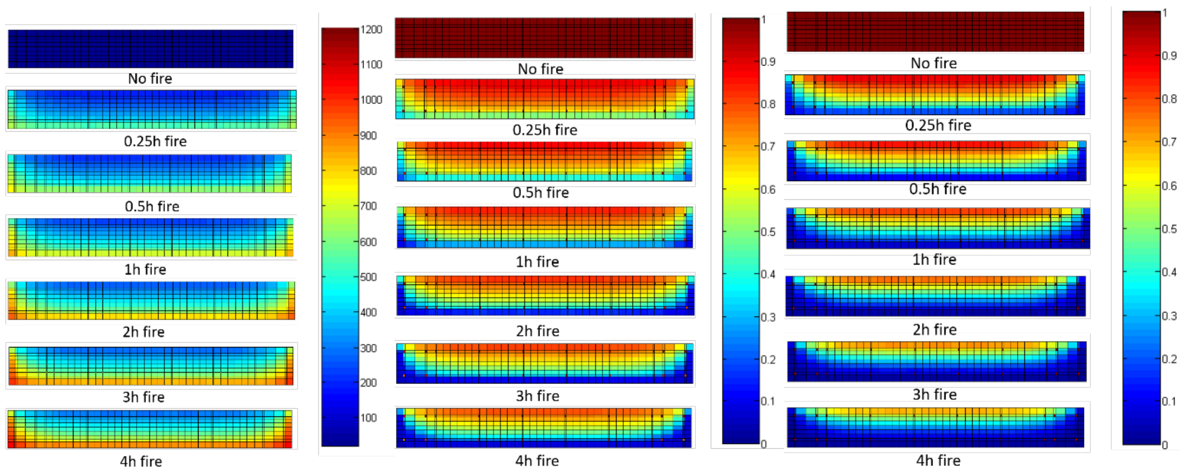

(a) Maximum temperature (T_{max}) (b) Residual strength ($f_{c,r}/f_{c,0}$) (c) Residual elastic modulus ($E_{ci,r}/E_{c,0}$)

Fig.3 – Temperature, residual strength and residual elastic modulus distribution of WR20 wall section

4. Evaluation of damage indices

Using the simulation procedure shown in Fig.1, the post-fire seismic performance of the sixteen walls listed in Table 1 is simulated under different fire durations. The response quantities, K_{sec} and V_{max} were taken from the load-drift response of walls under post-fire reversed-cyclic loads. Fig.4 shows the variation of DIEM and $K_{sec,fire}/K_{sec,0}$ with fire durations and the variation of DIS and $V_{max,fire}/V_{max,0}$ with fire duration for wall specimen WR20. The variation of the damage indices with fire duration based on Definition 1 is very similar to Definition 2. The variation of the damage indices with fire duration based on Definition 3 is very similar to that of Definition 4. These observations indicate the confining effect does not will not significantly influence the values of the damage indices. This observation is similar for the variation of damage indices with fire durations for the other fifteen walls. Therefore, only Definition 1 and Definition 3 were considered in the remainder of this paper.

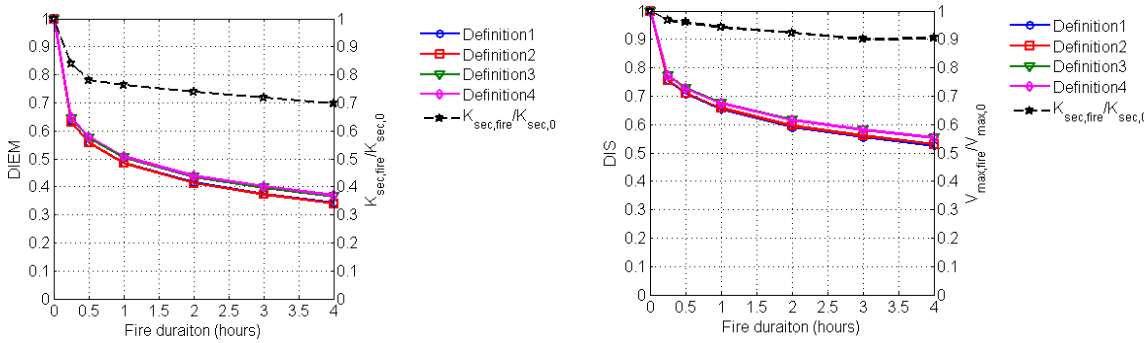

(a) 1-side fire

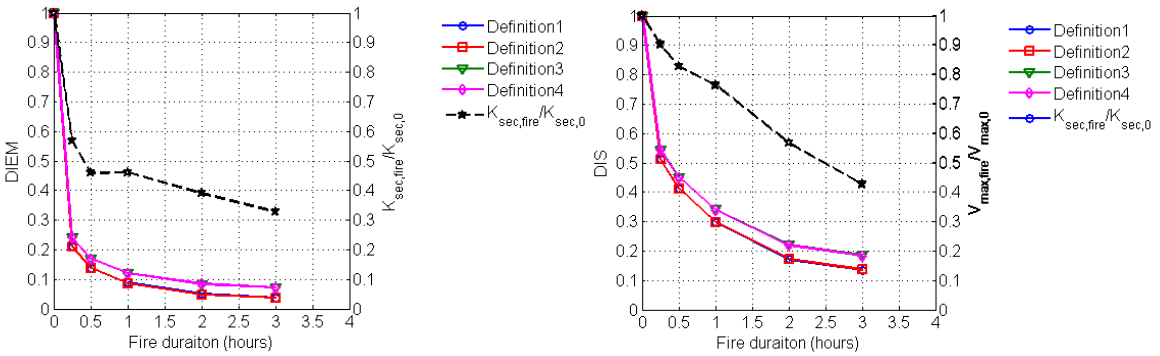

(b) 2-side fire

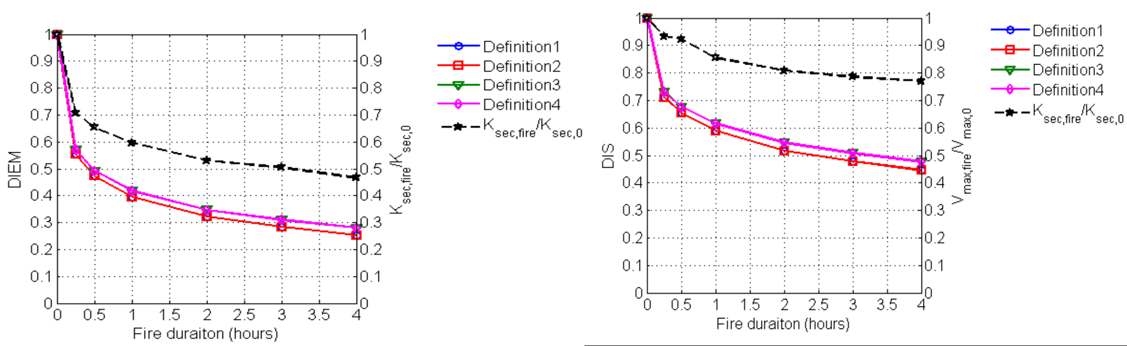

(c) 3-side fire

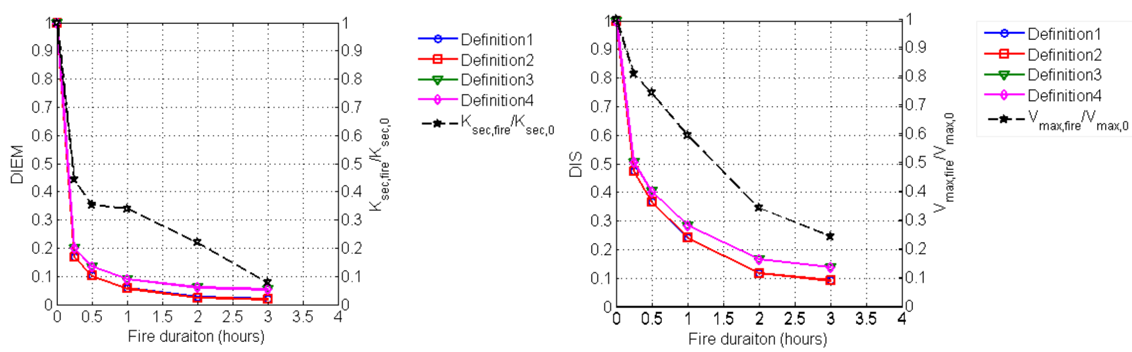

(d) 4-side fire

Fig. 4 – Variation of damage indices and wall response quantities with fire duration—Wall specimen WB20

5. Preliminary predication of wall responses based on damage indices

Fig.5 and Fig.6 show the variation of DIEM with $K_{sec,fire}/K_{sec,0}$ and the variation of DIS with $V_{max,fire}/V_{max,0}$ based on Definitions 1 and 3. At low damage indices, there is significant scatter in the reduction of strength and stiffness of the of the walls. Generally, this is the result of two- and four-sided fires (both long faces exposed), but not consistently; at low fire exposure times, such fires have damage indices similar to those for one- or three-sided fires at longer times, yet result in different stiffness and strength reduction ratios. At these low damage indices, the scatter is sufficiently large that such values will be excluded from the development of preliminary relationships for fire demand. The work in the following sections focus on DIS1 equal to or greater than 0.2, DIS3 equal to or greater than 0.3, DIEM1 equal to or greater than 0.15, DIEM3 equal to or greater than 0.2. An upper limit of the maximum damage indices investigated is applied in the relationships developed. More work is needed to investigate walls with larger damage indices; such values may be realistic with analysis of full-scale walls rather than test specimens.

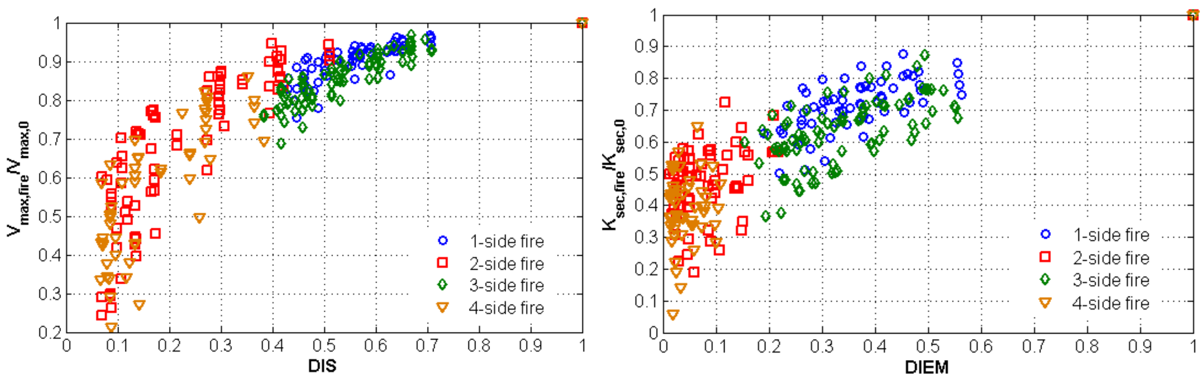

(a) $V_{max,fire}/V_{max,0}$ and DIS (b) $K_{sec,fire}/K_{sec,0}$ and DIEM

Fig. 5- Variation of $V_{max,fire}/V_{max,0}$ with DIS and $K_{sec,fire}/K_{sec,0}$ with DIEM based on Definition 1

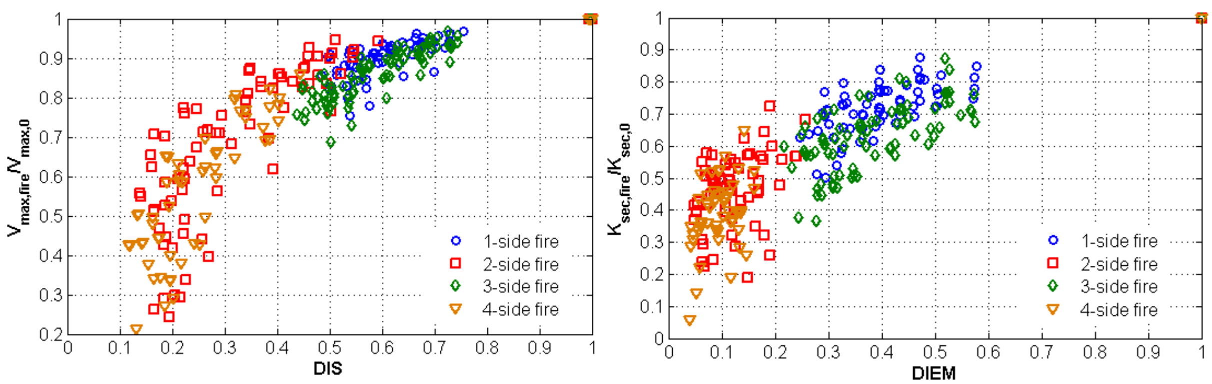

(a) $V_{max,fire}/V_{max,0}$ and DIS (b) $K_{sec,fire}/K_{sec,0}$ and DIEM

Fig. 6- Variation of $V_{max,fire}/V_{max,0}$ with DIS and Variation of $K_{sec,fire}/K_{sec,0}$ with DIEM based on Definition 3

Using these upper and lower bound limits, preliminary best fit relationships were established for the relationship between the damage indices and the wall response quantities. For Definition 1, these relationships are:

$$V_{max,fire}/V_{max,0} = 0.46DIS + 0.63 \quad (0.2 \le DIS \le 0.7) \tag{9}$$

$$K_{sec,fire}/K_{sec,0} = 0.61DIEM + 0.43 \ (0.15 \le DIEM \le 0.6) \tag{10}$$

For Definition 3, these relationships are:

$$V_{max,fire}/V_{max,0} = 0.44DIS + 0.61 \quad (0.3 \le DIS \le 0.75) \tag{11}$$

$$K_{sec,fire}/K_{sec,0} = 0.66xDIEM + 0.38 \quad (0.2 \le DIEM \le 0.6) \tag{12}$$

For each damage index value in Fig.7, the corresponding wall response ratios are not unique but have a range. For the safety of prediction, lower limits for the wall response ratios are preferred. The best fit relationships for the lower limits of Definition 1 are:

$$V_{max,fire}/V_{max,0} = 0.78DIS + 0.38 \quad (0.2 \le DIS \le 0.7) \tag{13}$$

$$K_{sec,fire}/K_{sec,0} = 0.90DIEM + 0.20 \quad (0.15 \le DIEM \geqslant 0.6) \tag{14}$$

For Definition 3, these relationships are:

$$V_{max,fire}/V_{max,0} = 0.77xDIS + 0.34 \quad (0.3 \le DIS \le 0.75) \tag{15}$$

$$K_{sec,fire}/K_{sec,0} = 0.85xDIEM + 0.21 \quad (0.2 \le DIEM \le 0.6) \tag{16}$$

Fig.7 and Fig. 8 show these lines within the limits used. The R^2 value for Eq.9 is 0.54 and the R^2 value for Eq.10 is 0.41. The R^2 value for Eq.11 is 0.52 and the R^2 value for Eq.12 is 0.43. Thus, the accuracy of Eq.9 is very similar to that of Eq.11 and the fitting accuracy of Eq. 10 is very similar to that of Eq.12. Compared to Definition 3, the calculation of damage indices based on Definition 1 is relatively easy since no material properties for residual reinforcing steel are required for the calculation of damage indices. Additionally, the slopes of those equations are similar, which means that damage indices based Definition 1 and Definition 3 are of similar sensitivity. Thus, damage indices based on Definition 1 are recommended for their easy estimation and reasonable accuracy. For the safety of prediction, the lower limits based on Definition 1 can be used in the assessment of the load-bearing capacity and stiffness of a fire-damaged wall under lateral loads.

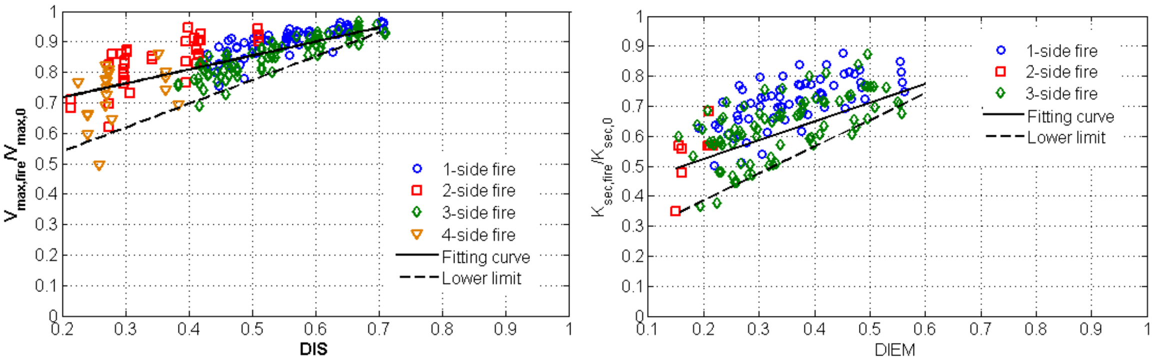

(a) $V_{max,fire}/V_{max,0}$ and DIS (b) $K_{sec,fire}/K_{sec,0}$ and DIEM

Fig. 7 – Fitting lines for the relationship between Vmax,fire/Vmax,0 and DIS and between Ksec,fire/Ksec,0 and DIEM (Definition 1)

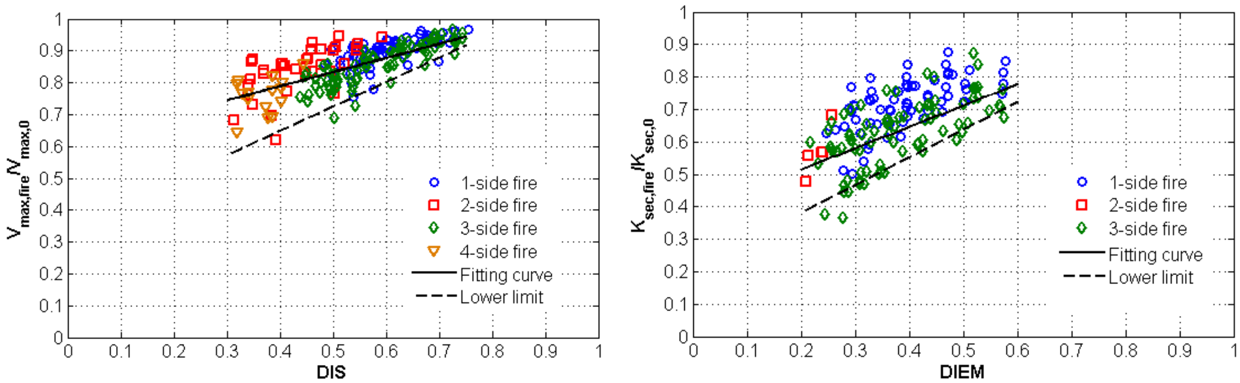

(a) $V_{max,fire}/V_{max,0}$ and DIS (b) $K_{sec,fire}/K_{sec,0}$ and DIEM

Fig. 8 – Fitting lines for the relationship between $V_{max,fire}/V_{max,0}$ and DIS and between $K_{sec,fire}/K_{sec,0}$ and DIEM (Definition 3)

6. Application of the damage indices

The reduction in the stiffness of RC shear wall is intended to account for the influence of concrete cracking, axial load, and reinforcing bond slip and anchorage extension. According to ACI318-11, the specified effective flexural stiffness E_cI_{eff} is 0.7 E_cI_g for uncracked walls and $0.35EcI_g$ for cracked walls. In order to further account the influence of fire exposure on the wall stiffness, the effective stiffness of cracked walls recommended by ACI318-11 could be further decreased by $K_{sec,fire}/K_{sec,0}$ (shown in Eq.10 or Eq. 12). The value of $K_{sec,fire}/K_{sec,0}$ can be calculated according to the damage index DIEM. For example, when the post-fire performance of a RC structural building is analyzed, the stiffness of fire-damaged walls can be further reduced according to the investigation of fire-damaged mateirals.

$$E_cI_{eff,fire} = K_{sec,fire}/K_{sec,0}E_cI_{eff} \tag{17}$$

When checking the strength of a fire-damaged wall, the normal strength of the fire-damaged walls can be obtained by multiplying the nominal shear strength of a RC walls with $V_{max,fire}/V_{max,0}$. The value for $V_{max,fire}/V_{max,0}$ can be calculated according to the damage index DIS of the wall section based on Eq. 9 or Eq. 11.

In some macro models of RC structural walls, the flexural behavior of walls is represented by springs. In order to account the influence of fire damage, the stiffness of those springs can be further reduced by the ratio of $K_{sec,fire}$ to $K_{sec,0.}$ The value for this ratio can be determined by Eq.9 or Eq. 10 and the damage index DIEM is determined based on the material degradation.

7. Conclusion

This paper proposed two simple fire damage indexes for reinforced concrete structural walls. One is for post-fire lateral-load capacity, DIS and another one is for the post-fire yield stiffness, DIEM. Four different definitions of the damage indices (DIEM and DIS) were proposed and compared. The simplest ones which only considered the residual material properties of concrete were recommended. The recommended damage index DIS is based on the residual compressive strength of concrete in a fire-damaged wall section and the recommended damage index DIEM is based on the residual elastic modulus of concrete in a fire-damaged wall section.

Numerical analysis of fire-damaged RC structural walls were conducted under reversed-cyclic loads. The values quantifying the damage indices and the wall performance were calculated. The relationships between the damage indices and the loading-bearing capacity and lateral stiffness of RC structural walls were developed. The R^2 value for the fit relationship between DIS and V_{max} is 0.72 and the R^2 value for the fit relationship between DIEM and K_{sec} is 0.81. The lower limits are also proposed for the relationships between damage indices and wall response quantities. Those fitting curves can be used by engineers or researchers to account the negative influence of fire damage to wall stiffness and wall strength under lateral loads.

Work is on-going to (i) model walls with dimensions for full-scale buildings, rather than scaled laboratory specimens and identify key characteristics impacting scatter in relationships presented here, (ii) propose improved damage indices for walls with that address both lower and higher damage indices; and (iii) propose the damage indices for the ductility and drift capacity of RC structural walls under reversed-cyclic loads and develop the relationships between the damage indices and wall ductility and drift capacity under reversed-cyclic loads.

8. References

[1] Ellsworth DE and Ginnado K (1991): Guide for visual inspection of structural concrete building components, USACERL Technical Report M-91/18, Construction Engineering Research Laboratory, US Army Corps of Engineers, July 1991

[2] Dilek, U (2007): Ultrasonic Pulse Velocity in Nondestructive Evaluation of Low Quality and Damaged Concrete and Masonry Construction, Journal of Performance of Constructed Facilities, 5(337), 337-344.

[3] Colombo M, Felicetti R (2007): New NDT techniques for the assessment of fire-damage concrete structures, Fire Safety Journal, 42,461-472

[4] Bungey JH, and Soutsos MN (2001): Reliability of Partially-Destructive Tests to Assess the Strength of Concrete on Site, Construction and Building Materials, 15, 81-92

[5] Eurocode 2 (2004): Design of concrete structures — Part 1–2: General rules — structure fire design., European Committee for Standardization, EN 1992-1-2

[6] ACI 216.1-97/TMS 0216.1-97: Standard Method for Determining Fire Resistance of Concrete and Masonry Construction Assemblies, ACI Manual of Concrete Practice Part 3 1998

[7] Andergerg, Y (1993): Computer simulations and a design method for fire exposed concrete columns. Report 92-50. Fire Safety Design, Lund, Sweden

[8] Franssen JM, Schleich JB, Cajot LG and Azpiazu W (1996); A simple model for the fire resistance of axially loaded members – comparison with experimental results, Constructional Steel Research, 37,3, 175-204

[9] Lie, TT and Irwin, RJ (1993): Method to calculate the fire resistance of reinforced concrete columns with rectangular cross section, ACI Structural Journal, 90, 1, 52-60

[10] Ni, S. and Birely, AC (2015): Post-fire earthquake resistance of reinforced concrete structural walls, Proceeedings of the 11th Canadian Conference on Earthquake Engineering, Victoria, July 21-24th, 2015

[11] Mazzoni, S, McKenna, F, Scott, MH and Fenves, GL (2006): OpenSees Command Language Manual", Pacific Earthquake Engineering Research Center, University of California, Berkeley

[12] Franssen, JM (2011): User Manual for SAFIR2011-A Computer Program for Analysis of Structures Subjected to the Fire, University of Liege

[13] Mazzoni, S, McKenna, F, Scott, MH and Fenves, GL (2006): OpenSees Command Language Manual, Pacific Earthquake Engineering Research Center, University of California, Berkeley

[14] Dazio A, Beyer K, and Bachmann H (2009): Quasi-static cyclic tests and plastic hinge analysis of RC structural walls, Engineering Structures, 31(7), 1556–1571

[15] Liu H (2004): Effect of concrete strength on the response of ductile shear walls, MS thesis, Dept.of Civil Engineering and Applied Mechanics, McGill University, Montreal, QC

[16] Lowes LN, Lehman DE, Birely AC, Kuchma DA and Marley KP and Hart CR (2012): Earthquake response of slender planar concrete walls with modern detailing, Engineering Structures, 43, 31–47

[17] Oh Y, Han S, and Lee L (2002): Effect of boundary element details on the seismic deformation capacity of structural walls, Earthquake Engineering & Structural Dynamics, 31(8), 1583-1602

[18] Thomsen J and Wallace J (2004): Displacement-based design of slender reinforced concrete structural walls–experimental verification, ASCE Journal of Structural Engineering, 130(4), 618-630

[19] Raghunandan M, Leil AB and Luco N (2015): Aftershock collapse vulnerability assessment of reinforced concrete frame structures, Earthquake Engineering & Structural Dynamics, 44, 419-439

[20] ACI, Building Code Requirements for Structural Concrete (ACI 318-11) and Commentary (ACI 318-11), American Concrete Institute, Committe 318, Farmington Hills, MI, 20011